

# Determining fracture toughness of polyethylene from fatigue

J. J. STREBEL, A. MOET

*Department of Macromolecular Science, Case Western Reserve University, Cleveland, OH, 44106*

A newly developed fatigue method of determining the value of the  $J$ -integral at crack initiation,  $J_{1c}$ , was tested on single-edge-notch-tension (SENT) specimens of a high-density polyethylene (HDPE). The fatigue method is able to propagate plane-strain brittle cracks in thin specimens which more closely approximate the "in-use" thickness, and hence the "in-use" morphology, of the polymer. This newly developed fatigue method was compared to ASTM standard procedure E813 (the ASTM method), which employs thick single-edge-notch-bend (SENB) specimens. Because of the similar size and shape of the crack-tip damage zone, the  $J_{1c}$  values for both methods were nearly identical ( $J_{1c} = 1.8 \text{ kJ m}^{-2}$ ,  $1.4 \text{ kJ m}^{-2}$  for the ASTM method and fatigue method, respectively).

## 1. Introduction

Load-bearing polymeric components are subject to a host of stresses which may vary in intensity and frequency over the lifetime of a structure. As a result of these varied stresses, small brittle cracks may initiate from surface scratches or internal flaws and slowly propagate. Eventually, these small propagating cracks will lead to the failure of the component. These brittle cracks are characterized by very small damage zones at the crack tip and macroscopically flat fracture surfaces. While these polymers may develop brittle cracks during use, in simple monotonic-tension tests the material can display a gradual yield and high elongation at break, i.e. ductile behaviour. Thus, an in-depth understanding of the resistance of ductile materials to brittle-crack initiation is critical to their use in engineering structural components which experience low stresses over extended periods of time.

One method which is often proposed to test the resistance of a ductile polymer to plane-strain brittle-crack initiation is given in ASTM procedure E813 (the ASTM method) [1]. Several attempts to measure the value of the  $J$ -integral at crack initiation,  $J_{1c}$ , of polymers have been made using the ASTM method, modifications of the ASTM method, and other  $J$ -integral methods. When alterations to the ASTM standard method are limited, values of  $J_{1c}$  for high-density polyethylenes (HDPEs) vary from 0.2 to  $2.5 \text{ kJ m}^{-2}$  [2-5].  $J_{1c}$  values for HDPE specimens in plane stress have been reported as high as  $185 \text{ kJ m}^{-2}$  [6]. In one case, a  $J_{1c}$  value of  $99.5 \text{ kJ m}^{-2}$  was reported for an ultrahigh-molecular-weight polyethylene (UHMWPE), but this high value was also believed to be caused by localized plane-stress conditions at the crack tip [7].  $J_{1c}$  is also sensitive to the strain rate of experiments. Varying the strain rate has caused HDPE  $J_{1c}$  values to vary from 1.6-40  $\text{kJ m}^{-2}$  [8]. In

the latter study, the ranking of different HDPEs, by their  $J_{1c}$  values, changed when the strain rate was varied [8]. Thus, for one type of material rather large fluctuations in  $J_{1c}$  have been recorded. Similarly, very large fluctuations have been noted in  $K_{1c}$ , a fracture-toughness parameter which is related to  $J_{1c}$  [9].

In addition to the effect of varied strain rates, different laboratories may employ dissimilar pre-cracking or notching methods, as well as different crack-extension measurement techniques. Variations in any of these factors can alter the  $J_{1c}$  value obtained. As a result, a great deal of caution must be exercised when comparing  $J_{1c}$  values reported from different laboratories. From a brief literature survey, it seems that many polymers have  $J_{1c}$  values in the same approximate range, i.e., 1-10  $\text{kJ m}^{-2}$  [5, 10-17]. The relatively small range of polymeric  $J_{1c}$  values, as well as the many factors contributing to the scatter of any one value, can make material differentiation on the basis of  $J_{1c}$  difficult. However, some intralaboratory material comparisons have been able to use  $J_{1c}$  to distinguish between different polymers [4, 18].

The ASTM method uses thick monotonically loaded specimens to determine the value of the  $J$ -integral at initiation,  $J_{1c}$ . For some materials, this method works very well. However, some tough resins do not initiate a brittle crack under the monotonic-loading conditions of the ASTM method, rather they fail by a ductile-yielding process. In addition, the very thick specimens required to produce plane strain by this method may have significant morphological differences from the thinner components into which the polymer is moulded for practical applications. Since fracture resistance is affected by morphology, this thickness difference may result in differences in fracture toughness between the specimen and the actual component.

These limitations can be overcome by our newly developed fatigue method of determining  $J_{1C}$ . This method applies the energy definition of the  $J$ -integral to a fatigue test. Using this technique,  $J_{1C}$  values are calculated which are similar to those obtained using the ASTM method. However, the fatigue method is able to produce brittle fractures in thin specimens of very tough materials. This paper reexamines the use of the ASTM method and introduces a new procedure, based on fatigue-crack propagation, which permits the calculation of  $J_{1C}$ .

## 2. Experimental procedure

### 2.1. ASTM method

Using thick compression moulded single-edge-notch-bend (SENB) specimens, the ASTM method was followed to determine the  $J_{1C}$  value of a HDPE. The SENB specimens were cut from 27 mm thick, compression moulded, plaques provided by Quantum Chemical Corporation. The specimen dimensions are shown in Fig. 1.

The specimens were fatigue precracked from a 17 mm deep machined v-notch until the fatigue precrack at midthickness was 19–27 mm long. The load during precracking cycled from 14–140 kg at a frequency of 0.5 Hz. After fatigue precracking, the specimen was allowed to relax for one day to minimize the residual stress effects of the precracking procedure. The actual test entailed monotonically loading the specimen at  $1 \text{ mm min}^{-1}$  until it was judged that crack growth had occurred. At that point, the specimen was unloaded at the same rate. The load–displacement plots were recorded during the monotonic loading and unloading periods.

In order to observe the crack-tip damage zone and to ascertain the crack-tip location, the unloaded specimens were cut in half along their midthickness. From one half of a specimen, thin sections were removed for transmission optical microscopy of the crack-tip region. The other half of the specimen was fractured at a high rate to reveal the fracture-surface features. Thus,

the crack extension,  $\Delta a$ , was determined with a high degree of accuracy. The  $J$ -integral was computed from the load–displacement curve (Section 3.1., 3.2.).

### 2.2. Fatigue method

Because of differences in morphology between thick specimens (ASTM method) and the thinner components of the polymer used in applications, it is desirable to be able to determine  $J_{1C}$  from specimens which approach the actual thickness in service. That is, in order to more accurately predict the fracture toughness of a loaded-polymer component, a fracture-toughness test should use specimens which are about the same size as the component, i.e. less than 5 mm thick. Therefore, from the same thick compression-moulded plaques of HDPE from which the ASTM specimens were cut, 4 mm thick single-edge-notch-tension (SENT) specimens were prepared.

The SENT specimens were notched by pressing a razor blade to a 5 mm depth; the specimen dimensions are shown in Figure 1. When properly fixed in the servohydraulic testing machine, 60 mm of specimen remained between the grips. The SENT specimens were fatigue loaded using a 0.5 Hz sinusoidal waveform to minimize hysteretic heating. The zero minimum load simplified the potential-energy measurement by eliminating the need for extrapolation to the  $x$ -axis (Sections 3.1., 3.3.). The maximum stress value,  $\sigma_{\max}$ , used in this study was 8.2 MPa, which is about 30% of the material yield stress. Stress levels at this percentage of the yield stress have previously been shown to produce brittle failure in reasonable testing times [19]. Load–displacement hysteresis loops were recorded on an  $x$ - $y$  plotter as the crack propagated. The crack-tip position was monitored with a travelling optical microscope. The crack extension was calculated as the difference between the growing crack length and the notch length.

## 3. Results and discussion

### 3.1. The $J$ -integral

The  $J$ -integral is a path-independent integral proposed by Rice [20] which describes the stress–strain fields at a crack tip. The magnitude of the  $J$ -integral at crack initiation,  $J_{1C}$  (the critical energy-release rate), is considered a measure of the fracture toughness of the material.  $J_{1C}$  is most commonly determined using the ASTM method, which was originally designed for metals, and it is now being sought for use with polymers. This method entails monotonic loading and unloading of the specimen, and the subsequent determination of  $J$  from load–displacement plots.

Because many plastics display ductile behaviour (i.e. large-scale yielding) under monotonic loading, it is necessary to make very thick specimens to constrain the plasticity at the crack tip and thus produce plane-strain conditions which initiate brittle cracks. The large specimen thickness required for the ASTM method severely restricts its usefulness, since moulding such thick specimens may be difficult, and since most polymeric components are too thin for direct testing.

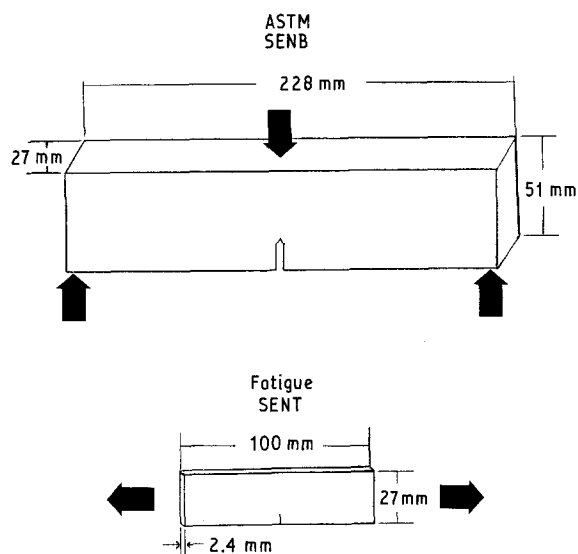


Figure 1 Geometries of the ASTM SENB and SENT specimens.

For an elastic body,  $J$  is equivalent to the energy release rate,  $G$ , and is defined as the change in potential energy,  $U$ , with respect to the change in crack length,  $a$ , per unit thickness,  $B$  [21]

$$J = -\frac{1}{B} \left( \frac{dU}{da} \right) \quad (1)$$

For compact-tension or bending specimens,  $J$  may be approximated using the area,  $A$ , under the load–displacement plot and the equation [22]

$$J = \frac{2A}{Bb} \quad (2)$$

where  $B$  is the specimen thickness, and  $b$  is the width of the stressed ligament. This calculation is illustrated in Fig. 2. Equations 1 and 2 are also valid for the elastic–plastic situation; however, in such a case,  $J$  may best be described as a measure of the stress–strain field near the crack tip [21]. Since  $J$  quantifies the deformation field at the crack tip, the value of  $J$  at the onset of crack initiation,  $J_{1C}$  may be used as a measure of fracture toughness.

### 3.2. ASTM method

Following the ASTM method, 14 specimens were monotonically loaded and unloaded, and  $J$  was calculated using Equation 2, as shown in Fig. 2. Ideally, each specimen would have experienced crack extension,  $\Delta a$ . However, measurable crack extension only occurred in 12 of the specimens.

After testing, each SENB specimen was cut in half at its midthickness plane. One half of the specimen was fractured at a high rate to reveal the fracture surface, while a section was cut from the other half for examination of the crack-tip profile. This sectioning technique was necessary because of ambiguous fracture-surface features (Fig. 3). Fig. 4 shows the crack profile and the accompanying half-fracture surface. Higher magnification of the crack tip revealed a small craze ahead of the crack tip. This craze is responsible for creating the extra band seen on the fracture surface (Figs 3–5). Without this type of careful microscopic analysis, it is possible to mistakenly include the craze in the crack-extension measurement and, as a result,

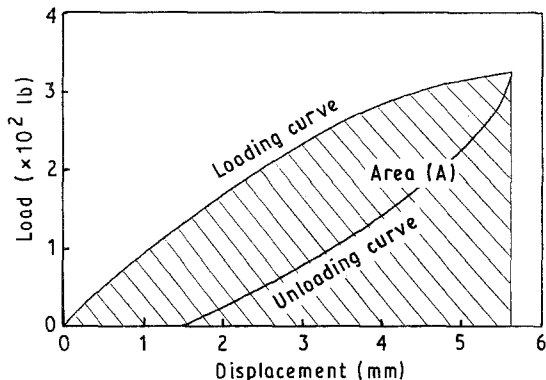


Figure 2 A ASTM SENB loading and unloading curve. The hatched area,  $A$ , is used to approximate the  $J$ -integral by  $J = 2A/(Bb)$ . Crack growth ( $\Delta a$ ) for this specimen was 2.9 mm.

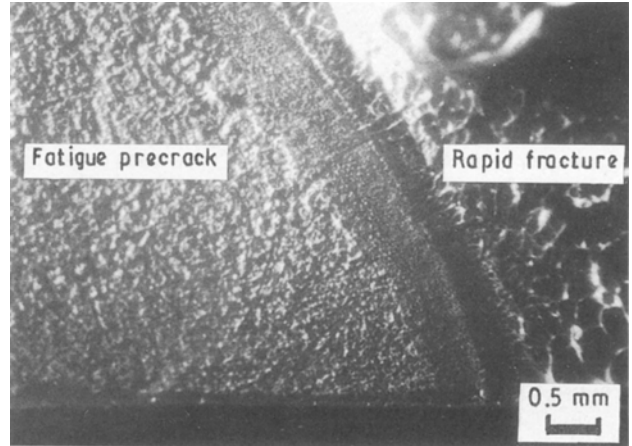
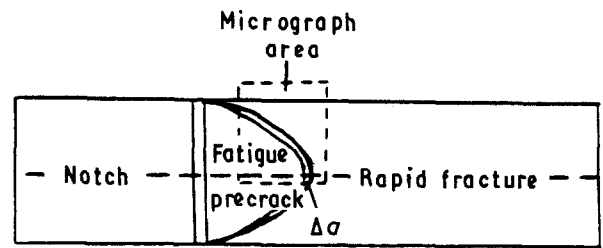


Figure 3 Area on the ASTM SENB fracture surface where crack growth occurred, showing ambiguous fracture-surface features between the precrack and rapid-fracture regions.

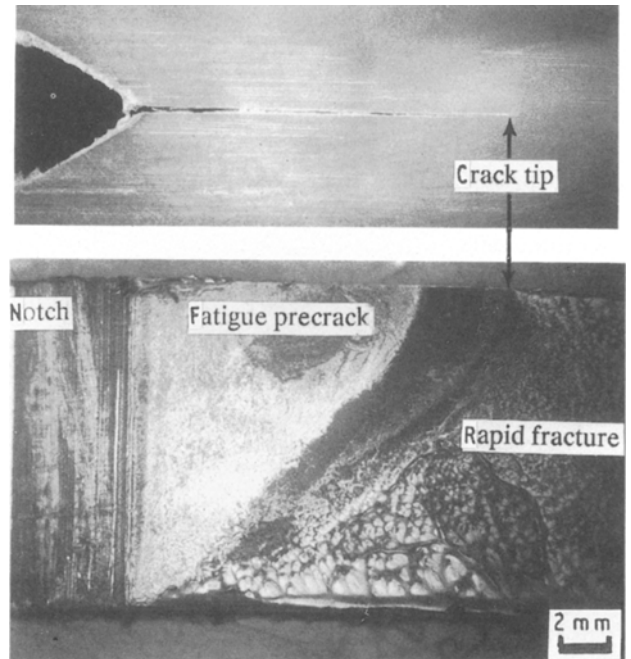


Figure 4 Comparison of partial ASTM SENB fracture surface and the corresponding crack profile used to identify the crack-tip position.

$J_{1C}$  will be underestimated. Likewise, Narisawa and Takemori have reported [10] the importance of positively identifying fracture-surface features before trying to measure crack extension.

After identifying the region of crack extension,  $\Delta a$  was recorded as the maximum crack growth within this region, as measured from optical micrographs. The ASTM method recommends averaging nine

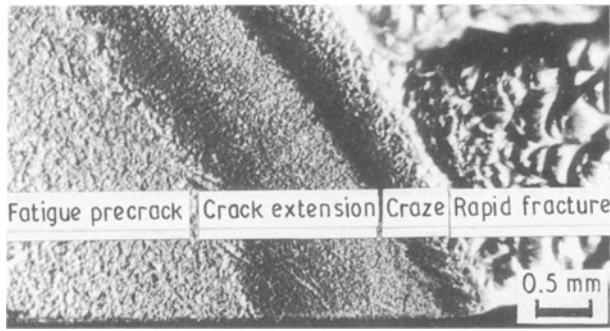


Figure 5 Partial ASTM SENB fracture surface with each area identified.

crack-growth measurements taken from the fracture surface. Because excessive crack tunnelling obscured the  $\Delta a$  region near the specimen edges, this nine-point technique was replaced by measurement of  $(\Delta a)_{\max}$ . Obviously, an averaging technique would produce lower  $\Delta a$  measurements and hence a steeper  $J$ - $R$  curve (higher  $J_{1C}$ ).

Having determined  $J$  and  $\Delta a$ , the data was plotted with the blunting line, and the 0.15 mm, 0.2 mm, and 1.5 mm blunting-line offsets (Fig. 6). According to the ASTM standard [1] the data which lies between the 0.15 and 1.5 mm blunting-line offsets (the dotted lines) is acceptable. Within this data window, the points must be distributed such that one point lies between the 0.15 mm blunting-line offset and a parallel line which intersects the abscissa at 0.5 mm. Another point must be located between the 1.5 mm blunting-line offset and a parallel line which intersects the abscissa at 1.0 mm. A minimum of four points are needed between the 0.15 mm and 1.5 mm blunting-line offsets. The seven filled symbols (■) in Fig. 6 meet these requirements.

This restricted data window is intended to select the region of crack growth in which  $J$ -integral analysis is valid. Data which falls to the left of the 0.15 mm blunting-line offset is excluded to prevent the inclusion of crack-tip stretch phenomena. Excluding data to the right of the 1.5 mm offset line ensures that any crack growth is within the zone of dominance of the crack-tip singularity fields [23]. This limit on crack growth helps to ensure that  $J$  is a unique measure of the stress and strain fields at the crack tip. However, the 1.5 mm blunting-line offset may be overly restrictive for bending specimens, since some tests suggest that crack growths of  $0.1b$  are acceptable [23]. For these tests, the  $0.1b$  limit would be near  $\Delta a = 3$  mm. Fig. 6 shows that the data (□) which are within the  $0.1b$  limit, but outside the 1.5 mm blunting-line offset, do follow the same trend established by the shorter  $\Delta a$  data, which fell within the restricted ASTM data window. Thus, in this case, a more liberal upper limit may be appropriate.

Using the present ASTM method (E813-87[1]), the acceptable  $J$  versus  $\Delta a$  data (■) fit a power-law curve (Fig. 6). This power-law regression fit was preceded in an earlier standard (E813-81) by a linear-data fit. The power-law fit more closely follows the actual data points, but it also tends to yield lower  $J_{1C}$  values than

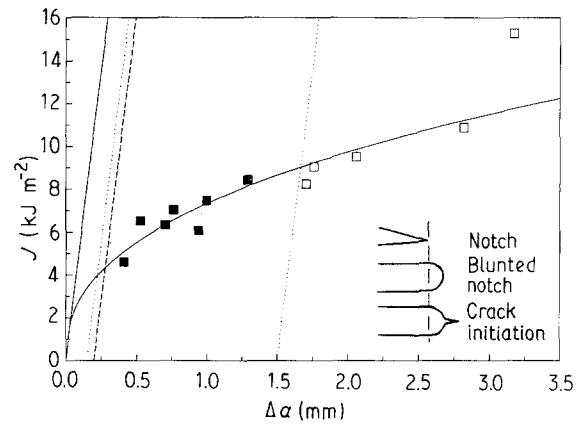


Figure 6 The  $J$ - $R$  curve for the ASTM method. The solid line through the data points is a power-law fit to the filled points. The unfilled points fall outside the ASTM data window. Blunting-line (—) offsets: (· · ·) 0.15 mm, (---) 0.2 mm, and (- · -) 1.5 mm. The insert shows the blunting phenomenon which is approximated by the 0.2 mm blunting-line offset.

the linear fit. This earlier version also specified  $J_Q$  as the intercept of the linear fit and the blunting line (solid line). In the present ASTM method [1], the intercept between the power-law fit (solid curve) and the 0.2 mm blunting line offset (dashed line) is termed the  $J_Q$  value (Fig. 6). Our  $J_Q$  value does not qualify as a valid  $J_{1C}$  value because of excessive crack tunnelling. Strict adherence to the ASTM method requires that of nine  $\Delta a$  measurements along the crack front, none differs by more than 7% from the average. On some specimens, we observed a difference of over 15%. Thus, we report a  $J_Q$  value of  $4.3 \text{ kJ m}^{-2}$ , rather than  $J_{1C}$ .

This value was determined by adherence to the standard, which assumes crack-tip blunting and thus employs use of the 0.2 mm blunting-line offset, which is simply a line parallel to the blunting line and which has been shifted 0.2 mm on the  $x$ -axis. The blunting line is described by the equation

$$J = 2\sigma_y \Delta a \quad (3)$$

where  $\sigma_y$  is the material yield stress. The use of the 0.2 mm blunting-line offset is meant to account for crack-tip stretch effects which may be observed prior to crack initiation, and be mistaken for crack growth. In some cases, loading of a sharp notch may produce a blunted notch with some apparent crack growth. From the blunted notch, a sharp crack may subsequently initiate (insert, Fig. 6). The 0.2 mm blunting-line offset is used to exclude the apparent crack growth due to blunting and thus approximate the location of crack initiation from the blunted notch. This blunting phenomenon is supported by some workers and opposed by others [4, 10, 24]. Later, the way the test conditions may determine whether or not such a mechanism occurs is described.

### 3.3. Fatigue method

Our recently developed fatigue method of determining  $J_{1C}$  is similar to the ASTM *single-specimen technique*. The ASTM single specimen technique follows the

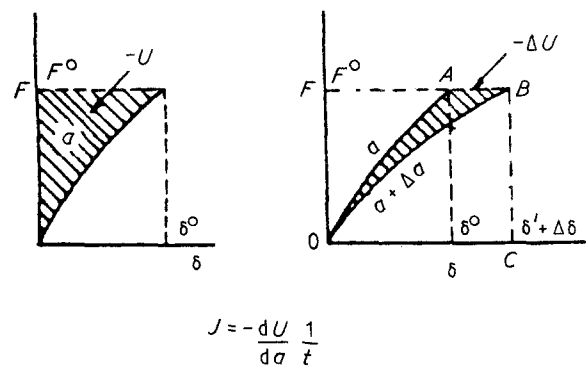
procedure of the multiple-specimen technique described above, except that, periodically during loading, the specimen is partially unloaded so that the crack length at that instant can be calculated from the slope of the unloading curve (compliance method). This technique enables several  $J-\Delta a$  points to be obtained from one specimen. This single-specimen method was originally applied to metals, which, because of minimal plasticity, only required slight unloading. However, because of increased crack-tip plasticity, the application of this method to tough polymers requires significant unloading to obtain an accurate assessment of the specimen's compliance from the curved unloading trace. For example, single-specimen testing of nylon was performed using a minimum-to-maximum load ratio of approximately two-thirds [25]. Because of the periodic unloading and reloading, the single-specimen technique is essentially a low frequency, high- $R$ -ratio ( $\sigma_{\min}/\sigma_{\max}$ ) fatigue test, while the fatigue method is a medium frequency, low- $R$ -ratio technique.

Previously,  $J$  has been determined (using Equation 2) during fatigue tests and the results can then be described by a Paris-type equation [26],

$$da/dN = C(\Delta J)^n \quad (4)$$

This suggests that  $J_1$  (or  $\Delta J_1$ ) plays a definite role as a driving force of propagating fatigue cracks, which implies that the crack-tip field, in fatigue, appears to be  $J$ -dominated. Thus, if  $J$  can be determined during fatigue-crack propagation, a  $J-\Delta a$  resistance curve may be constructed. Upon appropriate extrapolation of such a curve to the initiation point,  $J_{1C}$  may be obtained. Of course, a fatigue-testing window defining  $\sigma_{\max}$ , frequency, and specimen configuration ought to be defined. This window will be framed by the test conditions necessary to produce brittle-crack initiation and propagation in a reasonable time period.

Expanding on this idea, fracture toughness can be determined by applying the exact energy definition of the  $J$ -integral (Equation 1), rather than the approximation (Equation 2). According to this definition,  $J$  is proportional to the change in potential energy with crack growth, where the negative potential energy is the area above the load-displacement curve (Fig. 7) [21]. We recorded the load-displacement hysteresis loops while fatiguing SENT specimens, which were prepared from the same plaques as those used to prepare the ASTM SENB specimens. The area above the loading curve of the hysteresis loop is proportional to the negative potential energy of the specimen (insert, Fig. 8). The reproducibility of the fatigue experiment is shown in Fig. 8, where the negative potential energy is plotted as a function of the crack length for three identical tests. Due to the scale of the measured quantities, the differences shown between the three tests in Fig. 8 are minute. The differential of the fit to each set of negative potential energy versus crack length data will then be proportional to  $J$  (Equation 1). The change in crack length,  $\Delta a$ , during the fatigue test is equal to the crack length at any point minus the notch length.



$$J = -\frac{dU}{da} \frac{1}{t}$$

Figure 7 The area above the loading curve is proportional to the negative potential energy ( $-U$ ). As the crack grows from  $a$  to  $a + \Delta a$ , the area between the two loading curves is proportional to the change in potential energy,  $-\Delta U$ , associated with the increment of crack growth  $\Delta a$ , where  $t$  is the thickness. From: J. A. Begley and J. D. Landes, "The  $J$  Integral as a Fracture Criterion", ASTM STP 514 *Fracture Toughness* (American Society for Testing and Materials, Philadelphia, 1972) pp. 1-20.

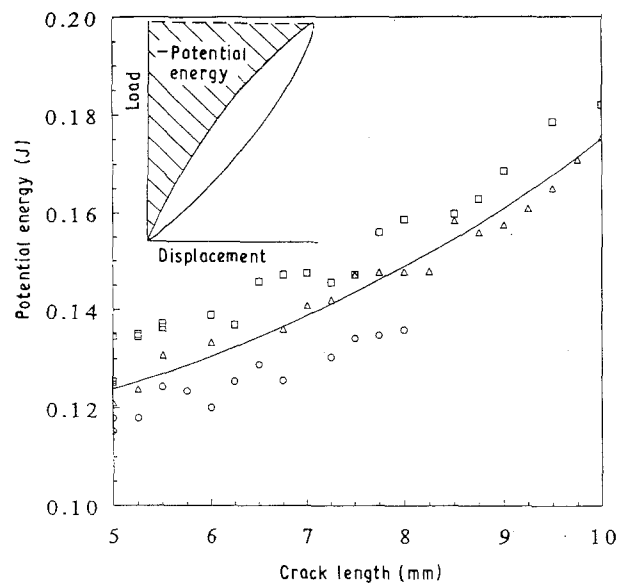


Figure 8 Evolution of the potential energy as a function of crack length during three fatigue tests.

The average  $J-R$  curve calculated from the three fatigue tests is shown in Fig. 9 along with the ASTM method  $J-R$  curve and the blunting line (Equation 3). The different slopes of the two  $J-R$  curves indicate a different resistance to continued crack propagation. Although crack-propagation resistance is a geometry-dependent phenomenon, one will note that the curves converge as the crack-initiation region (small  $\Delta a$ ) is approached. Fig. 9 is similar to behaviour observed by Begley and Landes [27] in which  $J_{1C}$  was determined for two different specimen geometries.

### 3.4. Determining $J_{1C}$

When the  $J-R$  curves have been generated by the ASTM method and the fatigue method, a  $J_{1C}$  value must be located on each curve. Since  $J_{1C}$  is the value of the  $J$ -integral at crack initiation, the crack-initiation point must be determined.

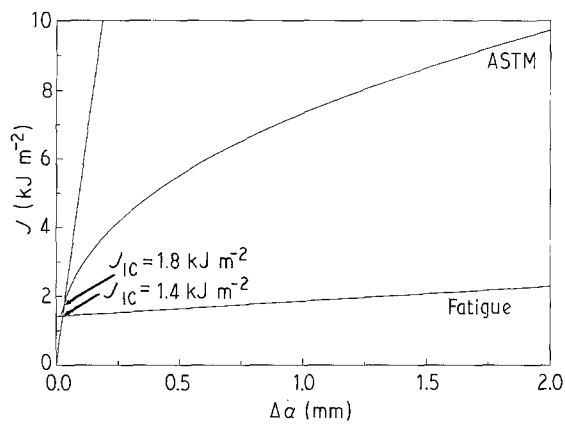


Figure 9  $J$ - $R$  curves for the ASTM and fatigue conditions for HDPE.

As previously discussed, the ASTM method [1] recommends using the point at which the  $J$ - $R$  curve intersects the 0.2 mm blunting-line offset. This technique is meant to account for crack-tip blunting effects (insert, Fig. 6). If the fatigue test is conducted at a higher stress level ( $\sigma_{\max} = 12.4$  MPa), crack blunting prior to initiation will occur (Fig. 10). In such a case, use of the 0.2 mm blunting-line offset would be appropriate. However, at the stress level at which this fatigue test was conducted ( $\sigma_{\max} = 8.2$  MPa), blunting is minimal (Fig. 11) and therefore the use of the blunting-line offset overestimates the amount of crack-tip stretch prior to initiation.

These initiation processes were visible because the fatigue specimens were only 4 mm thick. For the ASTM SENB specimen, the crack-initiation process could not be observed directly because the crack initiated in the centre of the 27 mm thick, opaque specimen. As an alternative to observing the crack at initiation, microtomed sections were removed from the thick ASTM SENB specimen after a crack had

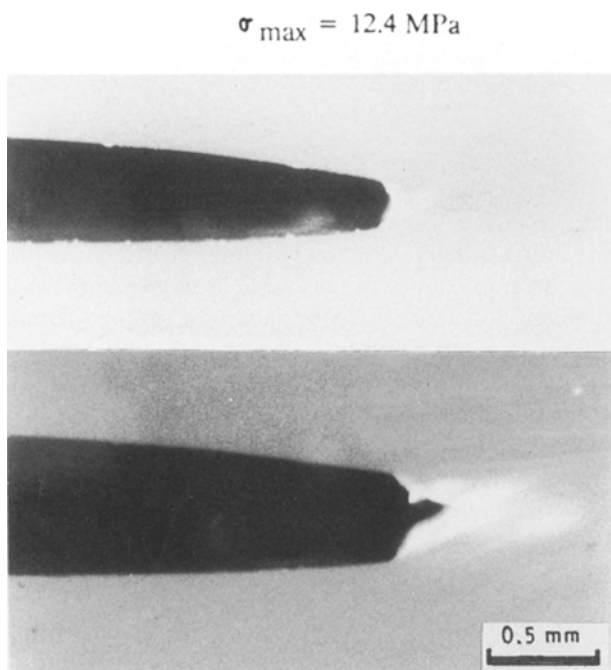


Figure 10 The crack-tip profile at initiation during a high-load-level fatigue test which shows the blunting phenomenon described in the insert in Fig. 6.

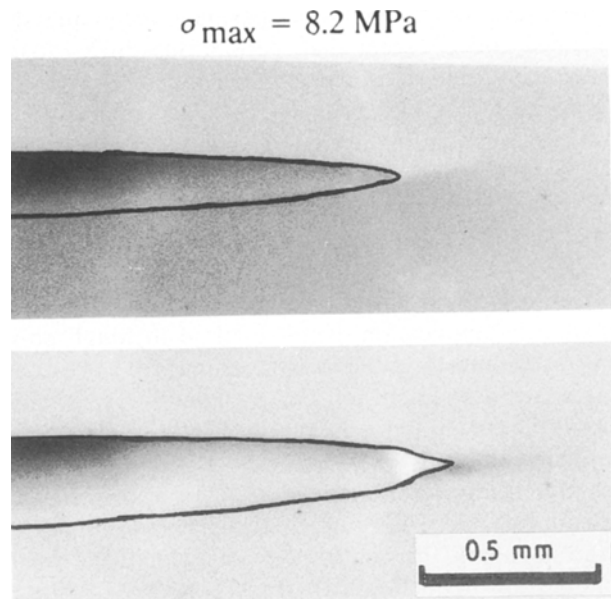
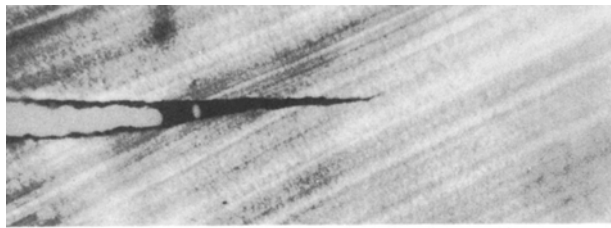


Figure 11 The crack-tip profile at initiation during the actual low-load fatigue tests. The crack profiles have been outlined.

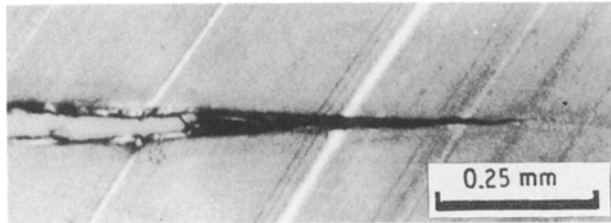
initiated. By comparing the crack profile of the SENB specimen to that of a fatigued SENT specimen which had a comparable crack extension, the relative difference in brittleness (plane-strain contribution) between the two specimens can be judged (Fig. 12). Although the SENB specimen does have a slightly larger craze than the fatigue SENT specimen, both cracks have a similar sharp appearance. Since it is known that blunting was minimal in the fatigue SENT specimen, we assume that it was also minimal in the ASTM SENB specimen because of the similarity in their crack-tip profiles. This conclusion negates the use of the 0.2 mm blunting-line offset and indicates that the initiation point for both specimens must lie to the left (smaller  $\Delta a$ ) of the 0.2 mm blunting-line offset.

Having discounted the use of the 0.2 mm blunting-line offset, a more accurate prediction of the crack-initiation point must be made. If it can be ascertained that absolutely no blunting occurred, the crack-initiation point would correspond to the  $y$ -axis ( $\Delta a = 0$ ). However, since some blunting has occurred (but much less than estimated by the 0.2 mm blunting-line offset) an initiation point between the  $y$ -intercept ( $\Delta a = 0$ ) and the 0.2 mm blunting-line offset would be appropriate. In addition, because a power-law regression fit was used for the ASTM data, choosing the  $y$ -intercept as the initiation criteria would always yield a  $J_{1C}$  of zero for the ASTM method. Thus, we believe the blunting line may be the best estimate of crack initiation for these experiments. However, under different loading conditions or different specimen geometries, it would be necessary to observe the crack-initiation phenomenon for each case and then determine the appropriate location on the  $J$ - $R$  curve which corresponds to  $J_{1C}$ .

The intersection of the  $J$ - $R$  curves with the blunting line indicates a  $J_{1C}$  of  $1.8 \text{ kJ m}^{-2}$  for the ASTM SENB specimen and a  $J_{1C}$  of  $1.4 \text{ kJ m}^{-2}$  for the SENT fatigue specimen (Fig. 9). These  $J_{1C}$  values are within the range for  $J_{1C}$  ( $0.2$ – $2.5 \text{ kJ m}^{-2}$ ) reported in the



Fatigue ( $\sigma_{\max} = 8.2\text{MPa}$ )



ASTM E813

Figure 12 Crack-tip profiles of interrupted fatigue and ASTM tests shortly after initiation.

literature for HDPEs [2–5]. Considering that these two methods differ in specimen geometry and specimen thickness, and that the two methods use very different loading conditions, the agreement between the two methods is excellent. This excellent agreement can be explained by the fact that  $J$  is a measure of the crack-tip deformation field, and since both methods have crack-tip damage zones of similar size and shape (Fig. 12), it was expected that they would have similar  $J_{1C}$  values.

### 3.5. Comparison of the ASTM and fatigue methods

As stated earlier this fatigue test can be conducted within a window of testing conditions which produce brittle fracture. In this case, the fatigue parameters were selected so as to mimic the fracture observed in the ASTM test. Both methods produced similar flat fracture surfaces and crack-tip damage zones of approximately the same size and shape. Excellent reproducibility can also be obtained with this method at different load levels [28]. However, higher loads produce larger crack-tip damage zones, and since the  $J$ -integral is a measure of the deformation at the crack tip, these higher loads yield higher  $J_{1C}$  values [28]. Others have also reported that  $J_{1C}$ , as determined by the ASTM method [1] varies with the loading conditions [8, 29]. The ASTM method was developed by simply constraining the test conditions. Similarly, the parameters of the fatigue method may be specified. In this case, the fatigue variables were set to produce a fracture similar to that observed by the ASTM method [1].

In addition to producing similar  $J_{1C}$  values to the ASTM method, the main advantage of the fatigue method is that it can be done with specimen thicknesses which more closely approach the thickness in which the polymer will be used. The ASTM method

requires thick blocks to constrain the ductility at the crack tip and thus produce a plane-strain brittle fracture, the worst-case-scenario. Whereas fatigue can be used on much thinner specimens to produce fractures which are even more brittle (higher-plane-strain contribution) than those observed by the ASTM method [28]. The primary importance of this advantage is quite simple. Because of differences in thermal history and processing methods (i.e., compression moulding or extrusion), differences in morphology arise between thick test specimens and the relatively thin components used in applications. These morphological differences affect fracture resistance. Thus, because of differences in morphology, the fracture resistance of a thick block specimen may not be an accurate measure of the fracture resistance of the actual thin component, even though both are made of the same material. However, if the fatigue method is used, specimens may be tested which approach the same thickness, and thus morphology, as real components. Testing these thinner specimens will give a more accurate assessment of the fracture toughness of the polymer part.

Another difference between the two methods is tied to the fact that, for some tough polymers, brittle cracks cannot be initiated using monotonic loading. For example, Crist and Carr have conducted  $J$ -integral studies on thick compact tension specimens of tough medium-density polyethylene pipe resins [30]. The “crack” which initiates is shown in Fig. 13. Under the conditions specified by the ASTM method [1] these materials separate by a tearing process which is accompanied by a large damage zone; they do not *crack* under monotonic load. Since a materials resistance to brittle failure is being tested, a test method which can produce a brittle crack is required. The SENT fatigue test can produce brittle failures in thin specimens of these tough resins, as well as provide  $J_{1C}$  values [31].

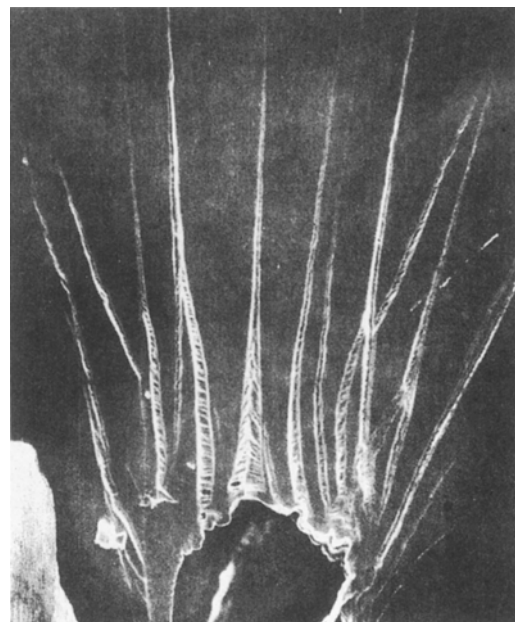


Figure 13 Crack tip-profile of an ASTM test in a tough, medium-density polyethylene [30].

The slow-crack-growth mechanism which produces these brittle failures is manifest by the size and shape of the crack-tip damage zone and by the fracture surface features. If the loading method, whether it be fatigue, monotonic, creep, or a combination of these types, produces the same fracture characteristics, then the mechanism of slow crack growth is the same. In this case, nearly identical features in HDPE are observed using either the fatigue or the ASTM method and thus that the fracture mechanism is nearly identical in both. Similarly, fatigue has also been used to produce features nearly identical to those observed in the field [32], and the equivalence of creep and fatigue loading has been documented previously [33].

Fracture-toughness testing of polymers requires constraining crack-tip plasticity in order to produce a plane-strain brittle fracture. This constraint can be accomplished by monotonically loading very thick specimens or by propagating a crack under the lower loads used in fatigue. In this case, we have selected fatigue conditions ( $\sigma_{\max} \approx 30\% \sigma_y$ , 0.5 Hz,  $R = 0$ ) which produce a damage zone which is roughly the same size as the damage zone in the ASTM test (Fig. 12); as a result, both  $J_{1C}$  values are similar. Regardless of the method,  $J_{1C}$  is a time-independent parameter which is being used to quantify fracture in a viscoelastic (time dependent) material. An improved measure of fracture toughness would incorporate both the time and energy necessary to fracture these materials.

#### 4. Conclusion

By applying the energy definition of the  $J$ -integral to fatigue tests, a method has been developed which permits the calculation of  $J_{1C}$  from thin SENT specimens. This method is capable of producing plane-strain brittle failures, characterized by small crack-tip damage zones and macroscopically flat fracture surfaces in thin specimens of tough polymers. The application of this newly developed fatigue method to HDPE has yielded a  $J_{1C}$  value ( $1.4 \text{ kJ m}^{-2}$ ) equivalent to that obtained using the ASTM method ( $1.8 \text{ kJ m}^{-2}$ ).

#### Acknowledgements

The support of the Gas Research Institute (GRI) under contract # 5083-260-2031 is gratefully acknowledged. The many helpful discussions with Dr Max Klein and Dr Kalyan Sehanobish, of GRI and Dow Chemical, respectively, are appreciated. Thanks is also due to Dr Buckley Crist and Dr Steve Carr, of Northwestern University, for sharing their unpublished data. The polyethylene specimens were generously supplied by Dr Koksai Tonyali of Quantum Chemical.

#### References

1. Annual Book of ASTM Standards, Vol. 3.01, E813 (American Society for Testing and Materials, Philadelphia 1988).
2. I. NARISAWA, *Polym. Engng Sci.* **27** (1987) 41.
3. B. CRIST and S. H. CARR, *Polymer* **32** (1991), 1440.
4. S. HASHEMI and J. G. WILLIAMS, *Poly. Engng Sci.* **26** (1986) 760.
5. Report on the ASTM Task Group Meeting on  $J$  Testing of Polymers, Orlando, FL, November, 1989.
6. Y. W. MAI, B. COTTERELL, R. HORLYCK and G. VIGNA, *Polym. Engng Sci.* **27** (1987) 804.
7. C. M. RIMNAC, T. M. WRIGHT, R. W. KLEIN, *ibid.* **28** (1988) 1586.
8. D. B. BARRY and O. DELATYCKI, *J. Appl. Polym. Sci.* **38** (1989) 339.
9. A. E. CHAMBERS and G. B. SINCLAIR, *Int. J. Fracture* **30** (1986) R11.
10. I. NARISAWA and M. T. TAKEMORI, *Polym. Engng. Sci.* **29** (1989) 671.
11. P. K. SO and L. J. BROUTMAN, *ibid.* **26** (1986) 1173.
12. J. M. HODGKINSON and J. G. WILLIAMS, *J. Mater. Sci.* **16** (1981) 50.
13. I. NARISAWA and H. NISHIMURA, *ibid.* **24** (1989) 1165.
14. Report on the ASTM Task Group Meeting on  $J$  Testing of Polymers, San Diego, CA, November, 1991.
15. Report on the ASTM Task Group Meeting of  $J$  Testing of Polymers, San Antonio, TX, November, 1990.
16. Y. W. MAI and B. COTTRELL, *Int. J. Fracture* **32** (1986) 105.
17. R. K. SINGH and K. S. PARIHAR, *J. Mater. Sci.* **21** (1986) 3921.
18. S. HASHEMI and J. G. WILLIAMS, *Plastics and Rubber Processing and Applications* **6** (1986), 363.
19. J. J. STREBEL and A. MOET, submitted to *Int. J. Fracture*.
20. J. R. RICE, *J. Appl. Mechanics* **35** (1968) 379.
21. J. A. BEGLEY and J. D. LANDES, *Fracture Mechanics*, ASTM STP 514 (American Society for Testing and Materials, Philadelphia 1972) p. 1.
22. P. C. PARIS, *Flaw Growth and Fracture*, ASTM STP 631, (American Society for Testing and Materials, Philadelphia 1977) p. 3.
23. J. W. HUTCHINSON, *J. Appl. Mechanics* **50** (1983) 1042.
24. D. D. HUANG and J. G. WILLIAMS, *Polym. Engng Sci.* **30** (21) (1990), 1341.
25. J. G. WILLIAMS, in Proceedings of How to Improve the Toughness of Polymers and Composites, October 8–11, 1990, Yamagata University, Yamagata, Japan (Yamagata University, Yamagata, Japan, 1990) 146.
26. N. E. DOWLING and J. A. BEGLEY, *Mechanics of Crack Growth*, ASTM STP 590, (1976) 82.
27. J. A. BEGLEY and J. D. LANDES, *Int. J. Fracture* **12** (1976) 764.
28. J. J. STREBEL and A. MOET, to be published.
29. R. E. JONES, Jr. and W. L. BRADLEY, "Fracture Toughness Testing of Polyethylene Pipe Materials", *Nonlinear Fracture Mechanics: Time Dependent Fracture*, Vol. 1, ASTM STP 995, 447.
30. B. CRIST and S. H. CARR, "Structural Basis for the Mechanical Properties of Polyethylenes", Gas Research Institute Annual Meeting, Chicago, IL, 9 May 1991.
31. J. J. STREBEL, "The Measurement and Origin of Fracture Toughness in Polyethylene", PhD thesis, Case Western Reserve University, Cleveland, OH, January 1993.
32. J. J. STREBEL and A. MOET, *J. Mater. Sci.* **26** (1991) 5671.
33. M. KLEIN, A. MOET and N. BROWN, Proceedings of the Society of Plastics Engineers Annual Technical Conference, Dallas, TX, May 1990, 1487.

Received 1 April 1992

and accepted 26 October 1992